Droplet Green Chemistry using Thermally Shape-Reconfigurable Omniphobic Colloidosome

Karan Jain,[a,§] *Saurav Kumar,*[a,§] *Manideepa Dhar,*[a] *Haydar Ali,*[b] *Nishanta Barman,*[a] *Debasmita Sarkar,*[a] *Mizuki Tenjimbayashi,*[*d] *Uttam Manna*[*a,b,c]

[*][a] Bio-Inspired Polymeric Materials Lab, Department of Chemistry

Indian Institute of Technology Guwahati, Kamrup,

Assam 781039, India

E-mail: umanna@iitg.ac.in

[b] Centre for Nanotechnology

Indian Institute of Technology Guwahati, Kamrup,

Assam 781039, India

[c] School of Health Science & Technology

Indian Institute of Technology Guwahati, Kamrup,

Assam 781039, India

[*][d] Research Center for Materials Nanoarchitectonics (MANA), National Institute for Materials Science (NIMS), Tsukuba, Ibaraki, Japan

E-mail: TENJIMBAYASHI.Mizuki@nims.go.jp

[§] Contributed equally.

Keywords: *: Omniphobicity • Droplet Green Chemistry • Colloidosome • Liquid marble• Shape-Reconfigurable*

Abstract:

A high-yield, lossless chemical reaction conducted under ambient conditions is promising in Green Chemistry. However, owing to the sticky feature of liquids on solid surfaces and the high volatility of useful primary solvents, "droplet chemistry" is far from practical use. Thus, a droplet platform that prevents both the droplet's evaporation and adhesion losses is promising. Herein, we report a versatile method for droplet encapsulation with poly octadecyl acrylate (PODAc) based on the colloidosome technique. The PODAc colloidosomes are mechanochemically stable and thermally shape-reconfigurable while maintaining their surface omniphobicity. This feature enabled PODAc colloidosomes to load typical liquids regardless of their surface tension without experiencing evaporation or adhesion loss, transport like solid beads, and release inner liquid on-demand by heating or NIR light irradiation. The colloidosome is mass-producible and recyclable by a simple thermomechanical process. As a proof-of-concept, different droplet-scale reactions are demonstrated in colloidosomes using volatile microliter solvent and volatile reactants.

1. Introduction

In 1998, Paul Anastas and John Warner manifested the 12 Principles of Green Chemistry. Briefly, waste-free, efficient chemical synthesis through catalysis or sustainable sources seems essential for the future of the chemical industry without additional energy input. Chemists and chemical engineers endeavoured to work on chemical processes with minimal synthesis cost. Ultimately, microlitre-scale chemical reactions may minimize the waste generated from such chemical processes and be helpful in the chemical processing of valuable reagents. However, it is known that droplets stick to the contacting media to minimize the total interfacial energy,[1] which results in adhesion loss of reactants−decreasing the reaction efficiency.

To address them, designing non-wetting interfaces around the droplet (for example, superhydrophobic,[2] superomniphobic,[3] slippery surfaces,[4-5] or liquid marble[6]) has been proposed to minimize adhesion loss, which has propelled sustainable chemical synthesis. Since the droplet levitation strategies, by heating, acoustic, or electric field,[7] require high energy input, there has been a notable focus on designing super liquid-repellent surfaces, especially in the recent two decades.[8-9] In Johnson and Dettre's study,[10] droplet sticking decreases with extreme roughening or sensitive smoothening of the interface. Thus, nano- and/or micrometer-scale roughened superhydrophobic or superoleophobic surfaces and nanometrically smooth lubricated[11] or solid-slippery surfaces[12] have been proposed to prevent loss of liquid because of droplets sticking to their contacting substrate. Further functionalizing these surfaces enabled

non-sticking droplet movement, and prototype chemical reactions by coalescing reactive droplets have been demonstrated.[13] These works proved that non-sticking surfaces can minimize adhesion loss. Especially, the recent progress enabled surfaces with non-sticking properties to low surface tension liquids.[5,14-15]

However, the inherent challenge in droplet chemistry has been ignored: "How to prevent droplets from evaporating ? " Primary organic solvents like acetone, ethanol, and hexane have high volatility. When the solvent evaporates, the chemical reaction becomes kinetically uncontrollable, and the target reaction efficiency suddenly decreases. This is because the solvent mediates the diffusion of reactive chemicals in the droplet. This solvent evaporation process renders droplet chemistry far from practical use. Ironically, the more the reaction volume is reduced toward Green Chemistry, the more the liquid vaporization effect cannot be ignored. Overall, preventing droplet sticking and evaporation simultaneously by generally applicable methods is critical in droplet green chemistry.

One approach is to encapsulate the liquid droplet inside liquid-repellent materials. The concept of covering the droplet with (super)hydrophobic nanostructure, namely liquid marble, has been reported.[6,16-17] However, the mechanically weak and discontinuous shell of liquid marble cannot prevent evaporation, as liquid molecules can escape from the air-exposed area and pores in the nanostructure, as depicted in Figure 1S and Table S1. The other possibility is to cover the droplet with a solid and continuous shell embedded with solid-slippery properties to prevent loss of liquid because of 1) liquid adhesion to the inner shell of the capsule/colloidosome and 2) evaporation of encapsulated liquid. In this context, different types of reported capsules or colloidosomes having continuous shells (Figure S1) mostly lack the following abilities: i) Repellence to low surface tension liquids; ii) Preventing evaporation of inner liquid; iii) On-demand extracting/adding liquids inside the shell; iv) Reconfigurability of shell, v) Tolerance to mechanical damages; and vi) Triggered release of inner liquid as summarized in Table S2. Generally, reported solid-slippery surfaces, formed by covalently grafting flexible polymer brushes or alkyl monolayers on nanometrically smooth surfaces, exhibit omniphobicity.[18-19] It is worth mentioning that the classic omniphobic properties have commonly been achieved by a silane condensation reaction with the assistance of high temperature.[12] It would be extremely challenging to cover droplets of a wide range of volatile/non-volatile liquids with such a solid-slippery coating—following condensing silane oligomers,[18-19] growing the framework materials at elevated temperatures,[20] etc. In this prospect, the challenge is forming a

mechanically stable, omniphobic, easily processable, and reconfigurable capsule with an on-demand liquid-insert/release function.

Herein, we report versatile droplet capsulation with poly octadecyl acrylate (PODAc): a thermoplastic solid-slippery polymer. Unlike other solid-slippery surfaces, the PODAc is processable with a melting temperature of nearly 51°C, while its surface exhibits omniphobicity and chemical stability to any solvents owing to the hexagonally packed hydrocarbon chains of the comb-like fluidic polymer.[21] In this work, we processed the PODAc capsule based on the "colloidosome " technique, which involves the coating of the liquid droplet with phase-transitioning hydrophobic polymer particles—followed by melting of polymer particles to achieve crystalline, solid, and continuous shell around the encapsulated liquid droplet. This process enabled the on-demand capsulation/extraction of various liquid droplets, regardless of their surface tension and volatility, without any loss. Also, the PODAc colloidosome can be recycled with a minimal thermomechanical process, which reduces the unwanted loss in chemical reactions. As a proof of concept, we have demonstrated highly efficient chemical reactions with highly volatile liquids of volume ~ 20 μL by developing the PODAc colloidosome.

Results and Discussions.

Design of Omniphobic Colloidosome

In our current design of thermally shape-reconfigurable omniphobic colloidosome, a thermoplastic comb-like polymer PODAc was synthesized by free radical polymerization of octadecylacrylate (ODAc) (Figure 1A) following our previous report.[21] The conversion of ODAc into PODAc was monitored with ATR-FTIR analysis, as shown in Figure 1B, where the IR peak for vinylic C-H deformation of acrylate moiety at 1407 cm^{-1} was significantly compromised with respect to another IR peak for stretching of carbonyl groups at 1720 cm^{-1} after free-radical polymerization of ODAc. This is because only the vinyl group was consumed during the free-radical polymerization of ODAc while the carbonyl group remained unaffected. After that, the differential scanning calorimetry (DSC) study of PODAc (M_n of 81.7 kDa) revealed the thermoresponsive behavior of the prepared polymer with a phase transition (solid to liquid phase) temperature of 51°C, as shown in Figure 1C.

Next, the PODAc capsule was processed based on the "colloidosome" technique, which is depicted in Figure 1D, E. Firstly, PODAc is ground to powder state, possessing very low

wettability (contact angle of 151°, Figure S2) to glycerol. Thus, PODAc powder is adsorbed on the droplet surface, forming a liquid marble instead of being dispersed in the glycerol droplet. The powder size is tunable with the grinding of the PODAc, and we confirmed that liquid marble is formed with PODAc powders of different grain sizes from 23 ± 1.1 μm to 477 ± 21.8 μm (Figure S3A-E). Next, the liquid marble was heated locally using NIR light to melt the PODAc powder around the glycerol droplet to form the PODAc shell. Here, the shell thickness increases (from 8.7 ± 0.5 to 125.1 ± 2.4 μm) with the grain size (23 ± 1.1 μm to 477 ± 21.8 μm) of the PODAc powder (Figure S4A-P). In this work, the shell thickness ranges from 8.7 to 125.1 μm. After that, the thermoresponsive property of the PODAc was strategically utilized to remove encapsulated glycerol from the PODAc shell by thermal poring (Movie S1). The glycerol was wholly removed from the capsule due to its liquid-repellent feature. Then, target chemicals or solvents were filled into the empty PODAc capsule, which we term the PODAc colloidosome. It can be utilized successfully as a versatile droplet green chemistry platform, and the proof of concept will be shown in the application section.

While most liquid marbles are fragile and easily break down under mechanical stimuli (Table S1),[22] the mechanical robustness of the prepared colloidosome can be tuned over a wide range from fragile to extremely robust depending on the shell thickness, which is confirmed by the impact and compression tests (see Methods and Figure S5A-E). Landau and Lifshitz's theory can explain increased mechanical durability with thickness.[23] Fragile colloidosomes can be used for the mechanical release of inner liquid, while tough colloidosomes can be used for thermal release. The most robust PODAc colloidosome with a size of ~ 3.2 mm and 125.1 μm shell thickness remains intact even after a fall from a height of 1.8 m under gravity (Figure S5A, Movie S2). Meanwhile, liquid marble prepared from the same PODAc powder is not able to sustain an impact of falling from a distance of 2 cm, as shown in Figure S6 (Movie S2). We also confirmed that the colloidosome is not cracked even after compression with 1.3 N force (Figure S5 C-E, Movie S3). Figure S7 quantifies the change in stress-strain properties of the prepared colloidosome with different shell thicknesses. As a result, the colloidosome with the thick shell can be picked up and rolled with bare fingers, as depicted in Figure S8.

This thickness-dependent mechanical response is due to the crystalline packing of the octadecyl moiety of the PODAc. The crystalline packing of PODAc is confirmed by X-ray diffraction (XRD) analysis (Figure 1F). The XRD peak at 21.6° revealed the hexagonal packing of the octadecyl group of PODAc in its powder and colloidosome form. However, in contrast

to PODAc powder, the colloidosome shell comprises a continuous crystalline network. After converting powdered PODAc into the colloidosome shell, a smooth and featureless topography is noted in the optical bright-field microscope image (Figure 1G, left panel). This smooth polymeric film displayed an intense birefringence of cross-polar light (Figure 1G), attributed to the existence of the crystalline network of the thermoplastic polymer (Figure 1F). The nanometrically smooth surface is required for PODAC to display omniphobicity. The colloidosome's inner shell has nanometric smoothness, as confirmed by the images of the field emission scanning electron microscope (FE-SEM) and atomic force microscope (AFM) (Figure 1H, I). The fibril domains appear due to the crystalline network in the colloidosome shell. Before studying the solvent sticking property on the prepared colloidosome, the chemical stability of powdered PODAc under different solvents was investigated. We found the prepared comb-like polymer remained insoluble in different commonly used organic solvents—having a wide range of surface tensions (72.8 mN m^{-1} to 17 mN m^{-1}), as shown in Figure 1J. Even the PODAc powder floated on the water pool, whether it was acidic (pH 1), basic (pH 14), or contained dissolved salt, for one month, demonstrating its chemical stability (Figure 1K).

Study of the Droplet Sticking Property

The PODAc shell is chemically stable to any commonly used solvents, which enables the encapsulation of various chemicals for a long time without any spillage (Figure 2A). The colloidosome retains its spherical shape even after decanting any target liquids, regardless of their volatility or surface tension (γ_{LV} = 17−72.8 mN m^{-1}). The sphericity of the PODAc is quantified with the static contact angle Θ (Figure 2B). Owing to the rigid PODAc shell, the colloidosomes exhibited $\Theta > 170°$ regardless of liquid surface tension, while conventional liquid-repellent interfaces (superhydrophobic, lubricated slippery, or solid slippery surfaces, and liquid marbles) exhibit surface tension-dependent Θ evolution (Figure 2C). For instance, a superhydrophobic surface repels high γ_{LV} liquid like water or glycerol with high Θ; however, it fails to repel low γ_{LV} liquids with low Θ. Similarly, the superhydrophobic PODAc powder (Θ=155 ° for water) failed to form liquid marbles with low surface tension liquids (Figure 2C and Figure S9). The Θ decreased with the γ_{LV} on perfluoropolyether-lubricated liquid slippery or PODAc-based solid slippery surfaces (Figure 2C). After that, we examined the adhesion force of colloidosomes filled with different liquids (range of surface tension from 72.8 mN m^{-1} to 17 mN m^{-1}) on a bare glass slide quantified by sliding angle α of 10 μL droplets.[24] The colloidosomes exhibit a sliding angle of $\alpha \approx 6-8°$, regardless of the liquid surface tension (Figure 2D), while other liquid-repellent surfaces partially failed liquid repellency. The

omniphobicity of the PODAc shell inner wall is critical to repeatedly replacing inner liquids from the PODAc colloidosome without fouling. The shell omniphobicity is estimated from the sliding angle on the PODAc solid-slippery surface in Figure 2D, which shows that all the probe liquids having γ_{LV} > 20 mN m^{-1} be easily removed. In this context, superhydrophobic and liquid-infused slippery interfaces repel only a few probe liquids with γ_{LV} > 50 mN m^{-1}, as illustrated in Figure 2D. Moreover, the surface tension of encapsulated liquid in liquid marble derived from superhydrophobic PODAc powder displayed a change in the sliding angle because of the alteration in the contact angle of liquid marbles on the solid surface. Despite the existing limitation of other bio-inspired interfaces, the currently developed colloidosome enables the no-loss transfer of a broader range of liquids compared to other liquid-repellent materials. It was noticed that the shape and contact angle of the colloidosomes merely altered on changing the volume of the inner liquid; however, the liquid marbles derived from superhydrophobic PODAc powder displayed a deformed shape and depleted contact angle on increasing the volume of the encapsulated liquid, as shown in Figure 2E-H. It is important to note that the thermal melting of deposited superhydrophobic PODAc powder on the encapsulated liquid has not only provided a crystalline network but also elevated the contact angle significantly at different volumes of encapsulated liquid. When the inner liquid volume is 30 µL, liquid marble is deformed by gravity, while colloidosome has high sphericity (Figure 2G, H).

It means that the thermal melting of the PODAc significantly elevated the contact angle. This encapsulation of different liquid types and volumes enabled a simple basis to encapsulate and store volatile/non-volatile chemicals in pre-defined volumes—without having any mass loss (Figure 2I). In this context, we can handle microlitter liquids like solid beads in containers without sticking or evaporation (discussed later), which would change the protocols of chemical synthesis. As a prototype demonstration, colloidosomes with different loading capabilities (2.5 µL to 10 µL) were successfully prepared by encapsulating various volatile and non-volatile liquids—including water, glycerol, DMF, and ethanol (Figure 2J-L). Such a non-sticking platform can handle tiny volatile and non-volatile liquids, which helps highly efficient droplet-based chemical reactions.

Study of the Droplet Evaporation

The PODAc colloidosomes can prevent inner volatile solvents from evaporation (Figure 3A and 3B). We selected water and hexane as probe volatile polar and non-polar liquids. The test

liquid volumes are 20 µL, and the water and hexane are dyed with methylene blue and Nile red, respectively. Time-lapse images of these liquid droplets in colloidosome compared with other liquid-repellent interfaces, including superhydrophobic, liquid-infused slippery, solid slippery surfaces and liquid marbles, are presented in Figure 3A, B. No changes in the PODAc colloidosome loaded with water and hexane are observed even after 8 h. In contrast, other liquid-repellent interfaces show droplet evaporation after a shorter duration. Even the shape and weight of water marble derived from powdered PODAc were observed to alter with time. To quantify the evaporation speed, we measured the weight change of the water and hexane droplet, depicted in Figure 3C and 3D. There is no significant weight change with time for the colloidosomes loaded with water or hexane droplets. Moreover, the water and hexane-encapsulated colloidosomes of crystalline shell displayed no change in shape and weight over 8 h—unambiguously suggesting no mass loss of volatile solvent from the prepared colloidosome. Similar results were obtained with different volatile solvents (ethanol and acetone), as demonstrated in Figures S10A and S10B. This perfect blocking property of inner liquid evaporation is due to the highly packed crystalline polymeric shell of the colloidosome. Irrespective of the nature of the encapsulated liquids, no noticeable change in shape and mass was observed for colloidosomes even after storing the colloidosome for a month (Figure S11).

The capsulation of the droplet with the PODAc shell lost the liquid diffusion property to the contacted media. However, taking advantage of the thermoresponsive behavior of PODAc, we successfully demonstrated the on-demand extraction of inner liquid and the addition of external liquids into the prepared colloidosome. The localized temperature-assisted formation of holes in the prepared colloidosome allowed the extraction of inner liquid and the addition of external liquid, respectively. Thus, while the closeness of the capsule prevents adhesion and evaporation, the reconfigurability of the same capsule shell allows on-demand addition and extraction of liquids. Moreover, the release of encapsulated liquids from the colloidosome is successfully depicted in Figure S12 and Figure S13. The liquid can be successfully released on both solid surface and liquid pools by applying either surface heating (Figure S12) or NIR light (Figure S13). In Figure 3F, the colloidosome was heated on a hot plate above 51 ℃ or irradiated with NIR light. We confirmed the release of water, glycerol, ethylene glycol, DMSO, DMF, acetone, ethanol, and hexane liquids as shown in Figure 3E, G. A similar outcome was observed on water or DMSO pools, as shown in Figure 3H. When the PODAc shell is heated above 51 ºC, the crystalline packing of PODAc is compromised. Thus, the phase transition of PODAc polymer at elevated temperature rapidly melted the shell of

collodosome to release the inner liquids on both solid surface and liquid pools (Figure S14). There is no difference in release mechanism of inner liquid from prepared colloidosome on both solid surface and liquid pools. Such on-demand, heat-triggered release of inner liquid from colloidosome would help to depict various on-demand chemical reactions. Further, the thermoresponsive character of the PODAc allowed the recycling of the PODAc shell to another fresh colloidosome (Figure 3I). After melting and releasing the inner liquid, we obtain the solid blocks of the PODAc. The block was processed into superhydrophobic powder by grinding, which enables the formation of the fresh colloidosome by repeating the formation process in Figure 1D-E. Thus, the current approach of preparing colloidosomes is also recyclable, as shown in Figure 3I.

Zero-loss Microreactor

In the history of droplet chemistry, liquid marbles were promising as a non-sticking platform for miniaturizing chemical reactions in microliter volume, where mostly non-volatile solvents (e.g., DMSO, DMF) are used as reaction medium.[25-26] However, uses of volatile organic solvents are rarely observed as the rapid loss of volatile solvents through unavoidable evaporation becomes exceedingly challenging. In this context, the prepared colloidosome that allowed evaporation-free, non-sticking encapsulation of various liquids with tunable volume has been successfully applied as a zero-loss microreactor to perform Schiff base reaction with a standard volatile organic solvent—i.e., ethanol in microliter volume over a relatively longer duration (Figure 4A-B). As a proof-of-concept demonstration, the prepared colloidosome was filled with an equimolar (0.1 M) amount of propylamine and vanillin in 20 mL ethanol, as demonstrated in Figure 4C. As the reaction proceeded, the reactants mutually reacted to form a Schiff base. Eventually, an intense yellow color was observed after a period of 1 h. The ATR-FTIR study of the reaction mixture encapsulated in colloidosome confirmed a complete conversion of reactants into the desired product, where the characteristic absorption peak of carbonyl (corresponding to aldehyde moiety of vanillin) at 1670 cm^{-1} was completely depleted—instead, a new absorption peak has appeared for imine stretching at 1640 cm^{-1} as shown in Figure 4E. Whereas in a controlled study, when the same reaction mixture was placed on a clean glass surface, a gradual loss of solvent was noted with time. Eventually, a dry and yellow color residue was found to be stuck on the glass slide, as shown in Figure 4D. Further, the ATR-FTIR analysis of solid residue on a glass substrate supports the incomplete reaction of the same reaction mixture. The characteristic absorption peaks for carbonyl and imine stretching were noticed at 1670 cm^{-1} and 1640 cm^{-1}, respectively (Figure 4E), suggesting partial

conversion of used reactants. The rapid evaporation of reaction media prior to the completion of the reaction is responsible for such incomplete chemical reactions. Thus, the prepared colloidosome can be successfully applied as a zero-loss microreactor, where the loss of solvent due to evaporation and the loss of product due to sticking on the solid surface can be avoided.

On-Demand Chemical Reaction

The on-demand chemical reaction is fascinating as the chemical reaction can be programmed as needed. However, the encapsulation and subsequent storing of volatile reactants for a prolonged duration—before their on-demand release to perform desired chemical reactions is challenging. In this context, bromine liquid—known to be a toxic chemical was encapsulated in a prepared colloidosome—and stored for 30 days, as shown in Figure 4F. No mass loss was noticed as the continuous crystalline network of prepared colloidosome is inherently capable of preventing the evaporation of volatile solvent and reactant. The thermo-responsive behavior of the prepared colloidosome that allowed the release of inner liquid at elevated temperature (> 51 ℃) was utilized to depict the on-demand interfacial reaction between phenol and bromine to form tribromophenol, as shown in Figure 4G-H. The encapsulated colloidosome was placed on an aqueous pool of phenol. Once the temperature of the aqueous pool was elevated above 51 ℃, the shell of the colloidosome melted, and the brown-colored bromine solution released into the aqueous solution of phenol to rapidly form a white precipitate of tribromophenol as shown in Figure 4I (Movie S4). ^{1}H NMR peak for ortho and para hydrogen at 6.8 ppm and 7.2 ppm of phenol diminished completely after the reaction. Additionally, the peak appearance and position for non-reactive meta hydrogen changes from triplet (6.9 ppm) to a singlet (7.5 ppm), confirming the successful bromination at the ortho and para position of phenol, as shown in Figure 4K. However, such an appearance of white precipitate was not observed on the release of the same bromine solution on a phenol-free water pool (Figure 4J). Hence, the current approach is not only capable of storing volatile reactants for a prolonged duration—but also the thermo-responsive nature of the prepared colloidosome enables the on-demand release of encapsulated volatile reagents to execute chemical reactions. Thus, the prepared colloidosome provided a much safer and greener platform for chemical reactions—even with toxic and volatile reagents.

Here, on-demand photopolymerization is demonstrated without releasing the inner reagents; instead, all the essential reactants were placed inside the colloidosome—and external stimuli, in that the chemical reaction is triggered by UV light. In this context, the UV light

transmittance (at a wavelength of 365 nm) of the PODAc shell was noticed to be increased by reducing its thickness, as shown in Figure S15A. The colloidosome with a shell thickness of 8.7 μm exhibited high UV transmittance (66%) and was used to encapsulate the monomer and initiator together to demonstrate on-demand photopolymerization through the UV irradiation process, as shown in Figure S15B, C. The photoreactive initiator (2-hydroxy-2-methylpropiophenone) provided reactive species to initiate the polymerization of glycidyl methacrylate (GMA)—and provided an epoxy group-containing chemically reactive poly glycidyl methacrylate PGMA. Reaction mixtures of monomer with different concentrations were loaded inside the colloidosome and exposed to UV light for 2 hours to allow polymerization reaction. In the end, the colloidosome was mechanically ruptured to get the resultant polymer, as shown in Figure S16E-G. Depending on the concentration of (0.75 M, 1.1 M, and 1.5 M) monomer, the molecular weight and the appearance of the resultant polymer in terms of its opacity and softness were altered. A brittle and solid polymer with M_n of 70.6 kDa was obtained at 1.5 M monomer concentration. In contrast, a semisolid transparent (M_n of 65.3 kDa) and opaque (M_n of 5.5 kDa) polymer was obtained at 1.1 M and 0.75 M, respectively. The complete polymerization of the monomer inside the prepared colloidosome was characterized with ATR-FTIR analysis, where the absorption peak for stretching of a vinyl moiety at 1637 cm^{-1} was diminished after the polymerization, as shown in Figure S15D. As expected, the IR signatures for the epoxy group were noticed at 907 cm^{-1}. Thus, the current approach allowed the on-demand synthesis of the chemically reactive polymer in an isolated and confined environment.

Chemical Reaction using Multi-fused PODAc Colloidosome

The spot melting of the PODAc shell enabled the interconnection of multiple colloidosomes, which makes the chemical reaction more systematic. In this section, we demonstrate the utilization of an interconnected network of colloidosomes for mixing solvents and chemicals. This is useful in depicting a programmed reaction, where multiple colloidosomes were connected through an inner hole to pass liquids. In the simplest model, two colloidosomes were fused thermally to achieve an interconnected passage for demonstrating liquid flow across colloidosomes, as shown in Figure 5A-B. Initially, the methylene blue-dyed liquid was introduced through the surface hole of one colloidosome, and this liquid flowed into the other connected colloidosome when the liquid level rose above the interconnected passage (Figure 5C and Movie S5). We utilized this principle for programmed reaction as schematically represented in Figure 5D, where four colloidosomes were interconnected with a central

colloidosome. After that, these four colloidosomes were pre-filled with different aromatic alcohols—including hydroquinone, catechol, phenol, and water- so their level remains below the interconnection pore to avoid backflow to the central colloidosome. Once the ferric chloride solution was passed through the inlet hole of the central colloidosome, it sequentially flowed to each of the connected colloidosomes via the interconnected pore, resulting in a change in the color of respective alcohols because of the formation of respective ferric complexes with aromatic alcohols (Figure 5E-F and Movie S6). This concept opened the possibility of systematic miniature chemical reactions. Recently, a complex fluidic device has been proposed based on complex geometric regulation of the liquid flow.[27-28] Recently, a high-resolution thermal patterning technique has also been reported.[29] Since the PODAc geometry is controllable with local heating, high-resolution thermal management may help to make the processing of PODAc colloidosomes more and more flexible. Owing to the facile processability and chemical stability, the PODAc colloidosome would be a powerful tool to customize droplet chemistry more efficiently and systematically. In the recent past, different and unique strategies, including spontaneous liquid flow reactors and cellular fluidics introduced to achieve rapid and controlled transport of liquids—but these approaches are with limited ability to prevent evaporation of volatile liquids.[30-31] In comparison, the current approach provided a facile basis for guided transport of wide range of liquids without mass-loss because of their evaporation and adhesion to the substrate.

Conclusion

In addition to the sticky feature of liquids (for example, sticking to a container), the high volatility of useful primary organic solvents restricts "droplet chemistry " from reaching its promising practical utilities. The dilemma is that the more the reaction volume is reduced, the more the vaporization effect of the liquid cannot be ignored. Here, we designed a thermally shape-reconfigurable omniphobic colloidosome that prevents both adhesion and evaporation losses of liquid species, thus acting as a powerful tool for droplet green chemistry. The novel feature of our approach is the molecular feature of PODAc's comb polymer structure: PODAc assembles to form a hexagonally packed hydrocarbon chain surface exhibiting omniphobicity and providing phase transition at a moderate temperature for shape reconfigurability. These features also help the easy and recyclable capsule shaping of the PODAc by adopting the colloidosome process. Our strategy is advantageous to classical omniphobic surfaces because of the broader range of surface tension of the repelling liquid, minimization of the liquid evaporation loss, and controlled release of the inner liquid. As a proof-of-concept, we show

four types of chemical reactions in colloidosomes with a volume of 20 μL solution of reactants: (i) long-time chemical reaction using volatile microliter solvent, (ii) on-demand release of volatile reactants to initiate a chemical reaction, (iii) on-demand photopolymerization in a confined space. The demonstration covers the typical prototype chemistry of molecular, polymer, particle, and catalytic reactions in droplet scale, which will be developed for more complex reactions using two or more PODAc colloidosomes using complex liquids. These applications prove that the PODAc colloidosome is inherently efficient for high-yield chemical reactions with valuable reagents and minimized waste. Higher-level processing, such as interconnected fused colloidosome capsules, would make chemical reactions more and more complex. As a laboratory glass instrument used for complex chemical reactions, the PODAc "vessel" processing would not be limited to the capsule shape for high-level green chemistry. However, the melting of colloidosome shell above the phase transition temperature of the PODAc makes it inappropriate to conduct isolated chemical reaction inside the colloidosome at elevated temperature. Hence, further development is required to improve the phase transition temperature of the comb-like polymer.

Supporting Information

The Supporting Information is available free of charge on the ACS Publications website.

Supporting information includes, materials, methods, additional experimental details on synthesis of polyoctadecyl acrylate, formation of colloidosome, refilling of empty colloidosome, tailoring of colloidosome shell thickness, compression test, droplet chemical reaction, programmed reaction. Figure S1-S15 accounting difference of liquid marble and colloidosome, contact angle of PODAc, size distribution of PODAc, shell thickness of colloidosome, stability of prepared colloidosome, change in contact angle with variation of surface tension of liquids, release of liquid from colloidosome on solid surface and liquid pool, on-demand photopolymerization. Table S1-S2 comparing the performance of prepared colloidosome over reported liquid marbles and capsules.

Author Contributions:

KJ and SK contributed equally to this work. KJ and SK: investigation, methodology, data collection, data analysis, validation, and writing & review; MD: methodology, investigating, data analysis, review and editing; HA: data collection, methodology, review and editing; NB: data collection and review; DS: data collection and review, MT: conceptualization, methodology, supervision, writing and review, UM: conceptualization, supervision, methodology, writing and funding acquisition.

Acknowledgements

UM thanks Science and Engineering Research Board (CRG/2022/000710), DBT (BT/PR45283/NER/95/1919/2022) and Ministry of Electronics and Information Technology

(no. 5(1)/2022-NANO) for financial support. UM thanks CIF, CFN, SHST and the Department of Chemistry, Indian Institute of Technology Guwahati, for their generous assistance in executing various experiments and for the infrastructures. SK, MD. NB thank the institute and Ministry of Education for PhD fellowship.

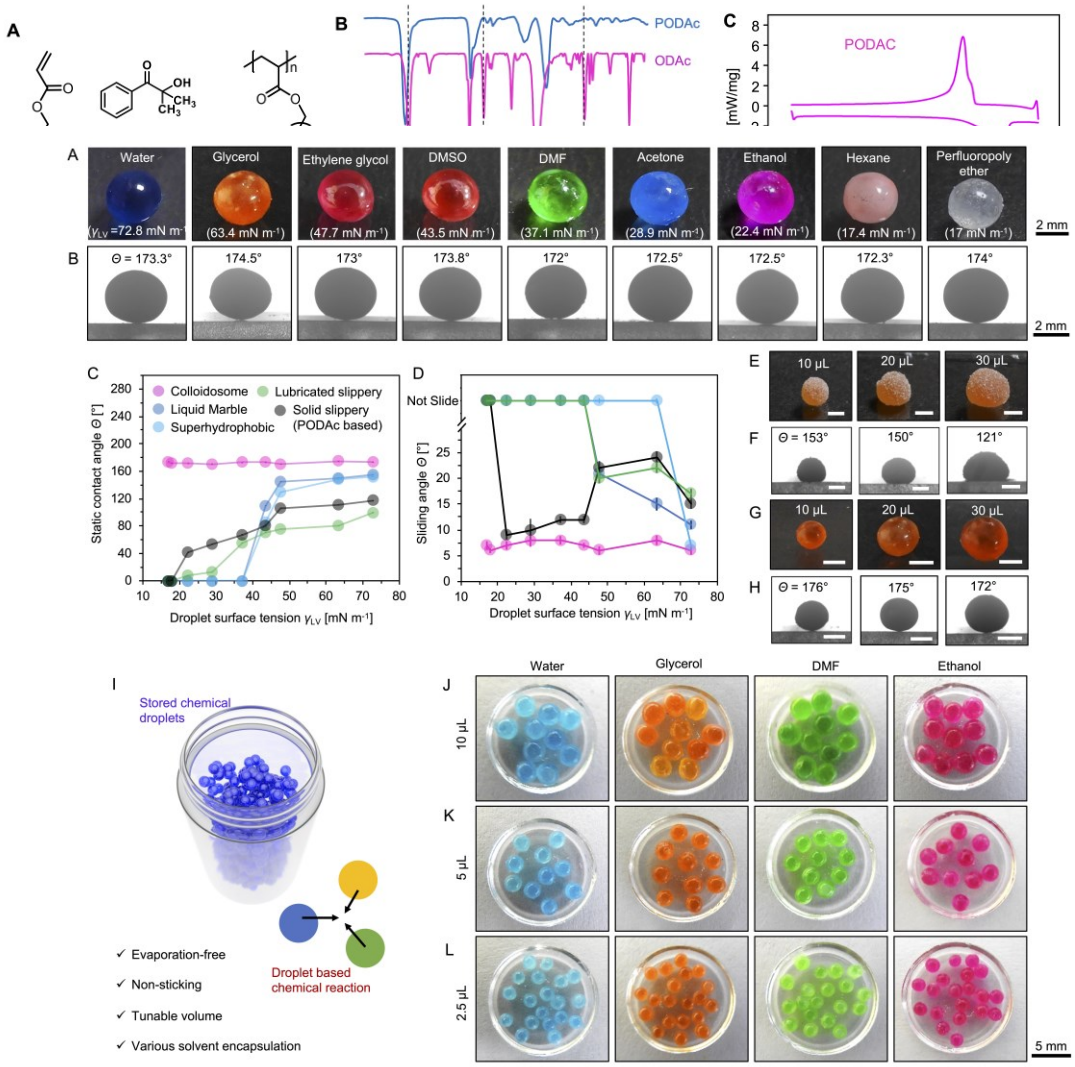

Figure 2. Liquid encapsulation in colloidosome. (A-B) Digital (A) and static contact angle (B) images of colloidosomes (volume = 20 µL) filled with different solvents having a wide range of surface tensions. (C) Graph showing the static contact angle values of different solvents used in encapsulating inside colloidosome on different interfaces including PODAc-based slippery coating, lubricated slippery surface, superhydrophobic interface, colloidosome and liquid marble. (D) Graph depicting the sliding angles of colloidosome filled with different solvents (volume of 10 µL) and liquid droplets (volume of 10 µL) of the corresponding solvents on a wide variety of selected interfaces. (E-H) Digital (E, G) and static contact angle (F, H) images of liquid marbles (E-F) and colloidosome (G-H) of different volumes (10 µL, 20 µL and 30 µL) of glycerol. (I) Schematic representation of colloidosomes storage. (J-L) Storing of colloidosomes of different volumes (10 µL, 5 µL and 2.5 µL) packed with different solvents. Results are presented as mean±SD, where sample size, n=3.

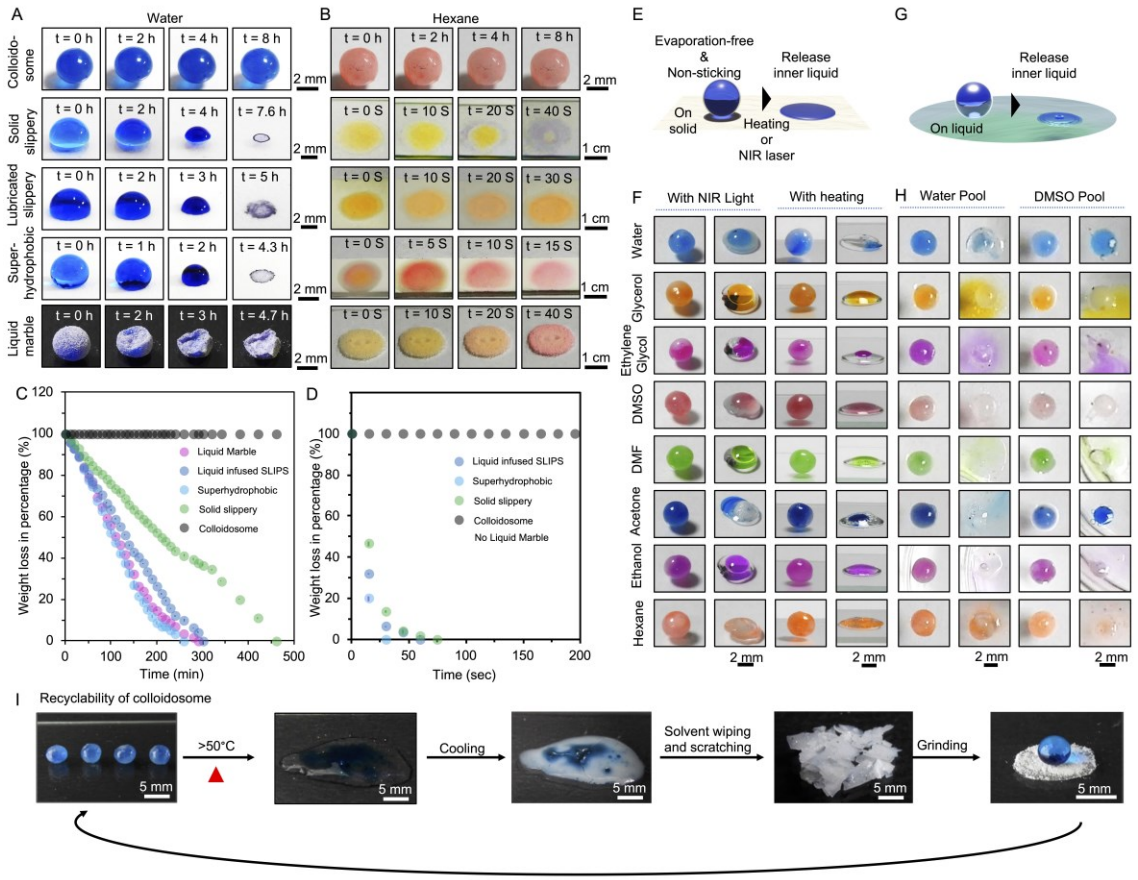

Figure 3. Evaporation tolerance and release of inner liquid. (A, B) Digital images comparing the evaporation of water (A) and hexane (B) droplets (volume = 20 μL) from different surfaces (solid slippery, liquid-infused SLIPS and superhydrophobic surfaces), liquid marble and colloidosome. (C-D) Graphical representation depicting the change in weight percentage of water (C) and hexane (D) droplets with time for different surfaces (solid slippery, liquid-infused SLIPS and superhydrophobic surfaces), liquid marble and colloidosome. (E) Scheme depicting the release of inner liquid from colloidosome on a solid surface upon heating. (F) Digital images showing the release of different solvents from colloidosome (volume = 20 μL) induced by heating with near-infrared (NIR) light and hot plate. (G) Schematic showing the release of inner liquid on a liquid pool upon heating. (H) Digital images representing the release of different solvents from colloidosome (volume = 20 μL) on water and DMSO pool induced by heating. (I) Digital images illustrating the recyclability of colloidosomes. Results are presented as mean ± SD, with a sample size of $n = 3$.

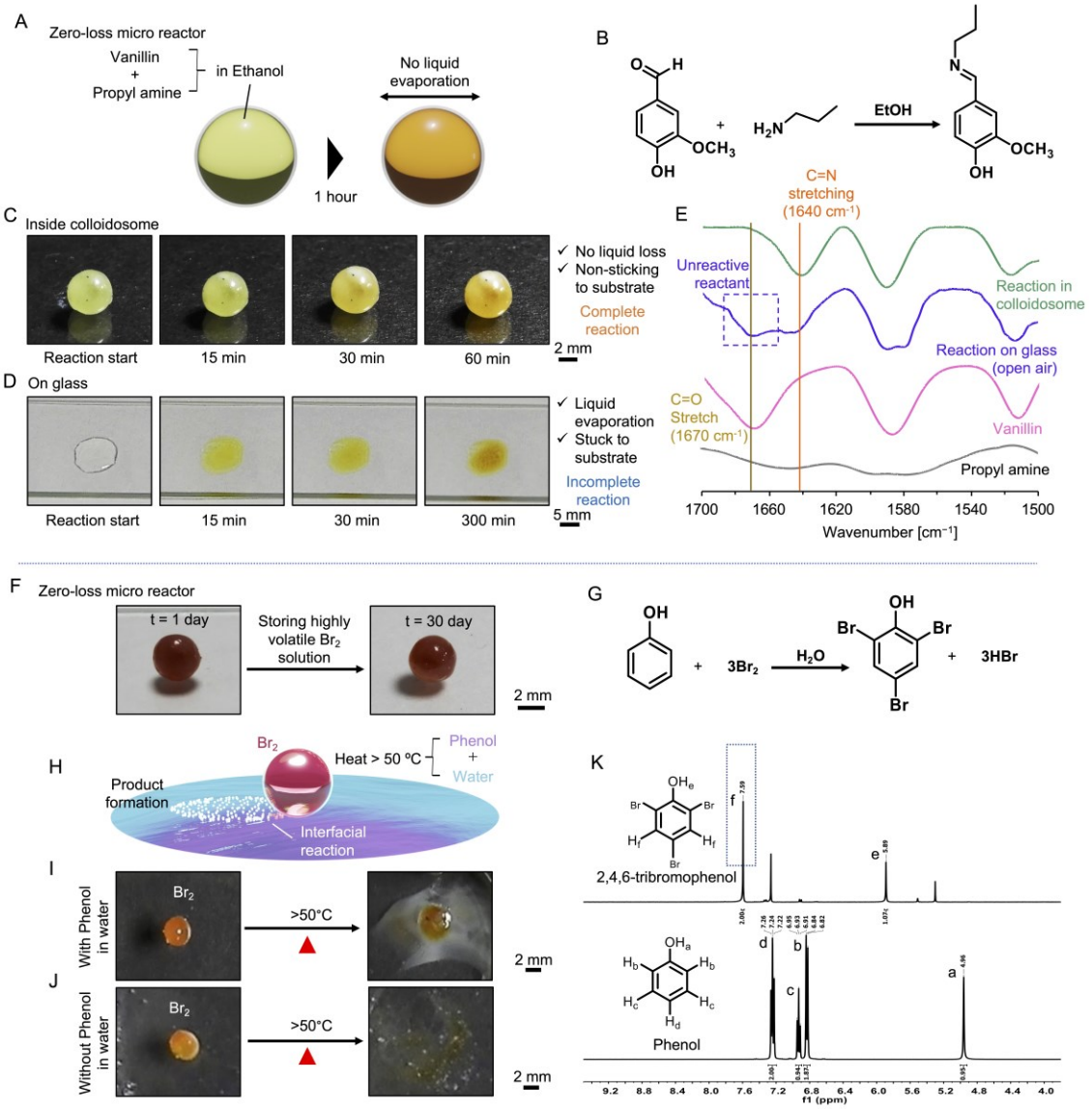

Figure 4. Chemical reaction using volatile reaction medium. **(**A-B) Schematic illustration of miniature Schiff-base reaction between (B) vanillin and propyl amine in a volatile organic solvent (ethanol). (C) Digital images showing the complete reaction of vanillin and propyl amine inside a packed colloidosome (volume = 20 µL). (D) Digital images showing the incomplete reaction between vanillin and propyl amine performed on an open glass substrate (volume = 20 µL). E) Attenuated total reflection-Fourier transform infrared (ATR-FTIR) spectra of vanillin (pink), propyl amine (grey), reaction mixture inside colloidosome (green) and on a glass substrate in open air (purple). Chemical reaction with volatile reactant. (F) Digital images depicting the storage of highly volatile bromine–water solution in colloidosome over 30 days. (G) Depicting the Bromination of phenol to form 2,4,6-tribromophenol. (H) Scheme representing the heat-induced release of bromine from colloidosome into aqueous solution of phenol resulting in the formation of 2,4,6-tribromophenol. (I) Digital images showing the release of bromine from colloidosome upon heating (volume = 20 µL) into an aqueous solution of phenol resulting in the formation of white-colored sediment. (J) H^1 NMR spectra of while sediment and phenol. (K) In the absence of phenol, no such changes were noticed even after the release of bromine from colloidosome (volume = 20 µL) upon heating into the water pool.

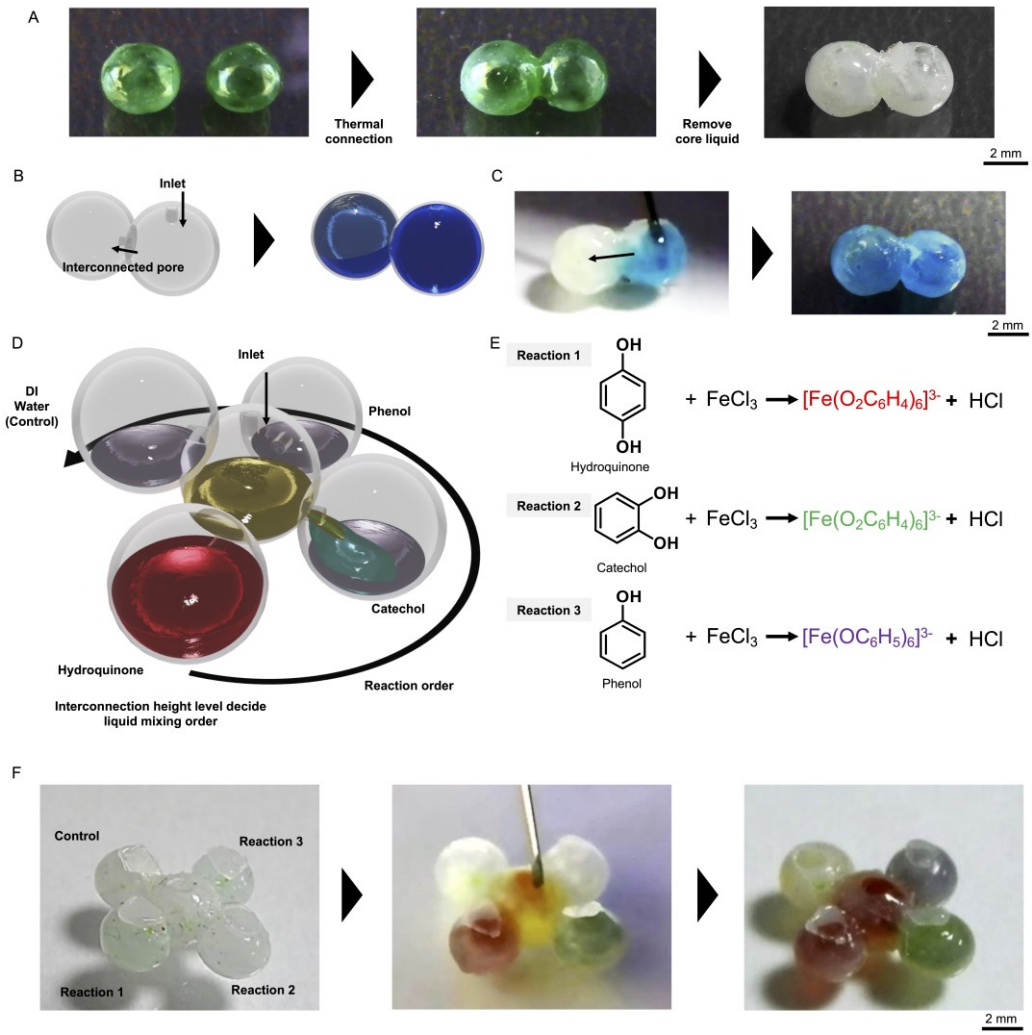

Figure 5. (A) Digital images depicting the steps involved in preparing a thermally fused empty colloidosome connected through a channel by joining two distinct colloidosomes filled with glycerol (volume = 20 µl), followed by decanting the glycerol from the fused state. (B-C) Schematic and digital images illustrating liquid (water dyed with methylene blue) flow from one colloidosome to another connected through a channel. (D) Schematic depicting the flow of ferric chloride solution from one colloidosome to four other connected colloidosomes containing hydroquinone, catechol, phenol, and distilled water. (E) Reactions of ferric chloride with different aromatic alcohols, including hydroquinone, catechol, and phenol, resulted in the formation of different complexes. (F) Digital images showing the flow of ferric chloride solution from one colloidosome to four other connected colloidosomes containing hydroquinone, catechol, phenol, distilled water, and the color change observed due to the formation of different complexes.

References.

(1) Young, T. An Essay on the Cohesion of Fluids. *Phil. Trans. R. Soc*. **1805,** *95*, 65-87.

(2) Onda, T.; Shibuichi, S.; Satoh, N.; Tsujii, K. Super-Water-Repellent Fractal Surfaces. *Langmuir* **1996,** *12*, 2125–2127.

(3) Tuteja, A.; Choi, W.; Mabry, J. M.; Mckinley, G. H.; Cohen, R. E. Robust Omniphobic Surfaces. *Proc. Natl. Acad. Sci. U.S.A* **2008,** *105*, 18200-18205.

(4) Wong, T.-S.; Kang, S. H.; Tang, S. K. Y.; Smythe, E. J.; Hatton, B. D.; Grinthal, A.; Aizenberg, J. Bioinspired Self-repairing Slippery Surfaces with Pressure-stable Omniphobicity. *Nature* **2011,** *477*, 443-447.

(5) Lafuma, A.; Quéré, D. Slippery Pre-suffused Surfaces. *EPL* **2011,** *96*, 56001.

(6) Aussillous, P.; Quéré, D. Liquid Marbles. *Nature* **2001,** *411*, 924-927.

(7) Ajaev, V. S.; Kabov, O. A. Levitation and Self-organization of Droplets. *Annu. Rev. Fluid Mech.* **2021,** *53*, 203-225.

(8) Dhyani, A.; Wang, J.; Halvey, A. K.; Macdonald, B.; Mehta, G.; Tuteja, A. Design and Applications of Surfaces that Control the Accretion of Matter. *Science* **2021,** *373*, eaba5010.

(9) Liu, M.; Wang, S.; Jiang, L. Nature-inspired Superwettability Systems. *Nat. Rev. Mater.* **2017,** *2*, 17036.

(10) Johnson, R. E.; Dettre, R. H. Contact Angle Hysteresis. III. Study of an Idealized Heterogeneous Surface. *J. Phys. Chem.* **1964,** *68*, 1744– 1750.

(11) Daniel, D.; Timonen, J.; Li, R.; Velling, S. J.; Aizenberg, J. Oleoplaning Droplets on Lubricated Surfaces. *Nat. Phys.* **2017,** *13*, 1020-1025.

(12) Chen, L.; Huang, S.; Ras, R. H. A.; Tian, X. Omniphobic Liquid-Like Surfaces. *Nat. Rev. Chem* **2023,** *7*, 123−137.

(13) Seemann, R.; Brinkmann, M.; Pfohl, T.; Herminghaus, S. Droplet Based Microfluidics. *Rep. Prog. Phys.* **2011,** *75*, 016601.

(14) Li, J.; Han, X.; Li, W.; Yang, L.; Li, X.; Wang, L. Nature-inspired Reentrant Surfaces. *Prog. Mater. Sci.* **2022,** *133*, 101064.

(15) Liu, T. L.; Kim, C.-J. C. Turning a Surface Superrepellent Even to Completely Wetting Liquids. *Science* **2014,** 346, 1096−1100.

(16) Aussillous, P.; Quéré, D. Properties of Liquid Marbles. *Proc. Math. Phys. Eng. Sci.* **2006,** 462, 973−999.

(17) Gallo, A.; Tavares, F.; Das, R.; Mishra, H. How Particle−Particle and Liquid−Particle Interactions Govern the Fate of Evaporating Liquid Marbles. *Soft Matter* **2021,** *17*, 7628−7644.

(18) Wang, L.; McCarthy, T. J. Covalently Attached Liquids: Instant Omniphobic Surfaces with Unprecedented Repellency. *Angew. Chem. Int. Ed.* **2016,** *55*, 244−248.

(19) Liu, J.; Sun, Y.; Zhou, X.; Li, X.; Kappl, M.; Steffen, W.; Butt, H. J. One-Step Synthesis of a Durable and Liquid-Repellent Poly(dimethylsiloxane) Coating. *Adv. Mater.* **2021,** *33*, 2100237.

(20) Singh, V.; Men, X.; Tiwari, M. K. Transparent and Robust Amphiphobic Surfaces Exploiting Nanohierarchical Surface-grown Metal-Organic Frameworks. *Nano Lett.* **2021,** *21*, 3480−3486.

(21) Dhar, M.; Das, A.; Parbat, D.; Manna, U. Designing a Network of Crystalline Polymers for a Scalable, Nonfluorinated, Healable and Amphiphobic Solid Slippery Interface. *Angew. Chem., Int. Ed.* **2022,** *61*, e202116763.

(22) Tenjimbayashi, M.; Fujii, S. How Liquid Marbles Break Down: Direct Evidence for Two Breakage Scenarios. *Small* **2021,** *17*, e2102438.

(23) Landau, L. D.; Lifshitz, E. M. Fluid Mechanics. *Cour. Theor. Phys.* **1986,** *109*, 3.

(24) Furmidge, C. G. L. Studies at Phase Interfaces. I. The Sliding of Liquid Drops on Solid Surfaces and a Theory for Spray Retention. *J. Colloid Sci.* **1962,** *17*, 309−324.

(25) Nguyen, N.-K.; Ooi, C.H.; Singha, P.; Jin, J.; Sreejith, K.R.; Phan, H.-P.; Nguyen, N.-T. Liquid Marbles as Miniature Reactors for Chemical and Biological Applications. *Processes* **2020,** *8*, 793.

(26) Xue, Y.; Wang, H.; Zhao, Y.; Dai, L.; Feng, L.; Wang, X.; Lin, T. Magnetic Liquid Marbles: A "Precise" Miniature Reactor. *Adv. Mater.* **2010,** *22*, 4814−4818.

(27) Yafia, M.; Ymbern, O.; Olanrewaju, A. O.; Parandakh, A.; Kashani, A. S.; Renault, J.; Jin, Z.; Kim, G.; Ng, A.; Juncker, D. Microfluidic Chain Reaction of Structurally Programmed Capillary Flow Events. *Nature* **2022,** *605*, 464−469.

(28) Zeng, C.; Faaborg, M.W.; Sherif, A.; Falk, M. J.; Hajian, R.; Xiao, M.; Hartig, K.; Bar-Sinai. Yohai.; Brenner, M. P.; Manoharan, V. N. 3D-printed Machines that Manipulate Microscopic Objects using Capillary Forces. *Nature* **2022,** *611*, 68-73.

(29) Durdevic, L.; Robert, H. M. L.; Wattellier, B.; Monneret, S.; Baffou, G. Microscale Temperature Shaping Using Spatial Light Modulation on Gold Nanoparticles. *Sci. Rep.* **2019,** *9*, 4644.

(30) Cao, M.; Qiu, Y.; Bai, H.; Tian, Y.; Wu, Y.; Jiang, L. Universal Liquid Self-transport Beneath a Flexible Superhydrophilic Track. *Matter*, **2024**, doi.org/10.1016/j.matt.2024.04.037.

(31) Dudukovic, N. A.; Fong, E. J.; Gemeda, H. B.; DeOtte, J. R.; Cerón, M. R.; Moran, B. D.; Davis, J. T.; Baker, S. E.; Duoss, E. B. Cellular Fluidics, *Nature*, 2021, 595, 58-65.

TOC Use only: